How Does Bovine Serum Albumin Prevent the Formation of Kidney Stone? A Kinetics Study

Junfeng Liu, Huaidong Jiang, and Xiang-Yang Liu*

Department of Physics, National University of Singapore, 2 Science Drive 3, Singapore 117542

Received: December 20, 2005; In Final Form: February 27, 2006

To attain a better understanding of the crystallization of calcium oxalate crystals under the influence of the protein bovine serum albumin, we examined not only the nucleation kinetics but also the structural synergy between the biomineral and the biosubstrate. It follows that during the crystallization process of calcium oxalate crystals bovine serum albumin inhibits the nucleation of calcium oxalate by increasing the kink kinetics barrier. The results of scanning electron microscopy and X-ray diffraction show, however, that bovine serum albumin promotes the formation of calcium oxalate dihydrate. Apart from this, bovine serum albumin facilitates the ordered calcium oxalate crystal assembly by suppressing the supersaturation-driven interfacial structure mismatch. The physics questions behind the mentioned effects have been addressed from the kinetics point of view. This may explain why bovine serum albumin plays an important role in suppressing urine stone formation.

Introduction

Calcium oxalate monohydrate (COM) is the main inorganic constituent of kidney stones.[1−6] The cost of the treatment for human kidney stone disease in the United States is estimated to be more than 2.4 billion dollars per year.[4,6] Thus, the study of calcium oxalate crystal (CaOx) formation is of major importance for human health. In particular, a fundamental understanding of the crystallization is essential for the study of micro-/nanostructure materials that have significant implications for life sciences.[3,4,6,7] Urinary proteins, such as the Tamm−Horsfall protein,[8−10] nephrocalcin,[11−13] osteopontin,[14−18] and human serum albumin,[3,7,14,19] are believed to have the potential to influence the crystallization of calcium oxalate. Among them, albumin seems to play a crucial role in kidney stone formation.[3,7,10,14,19−21] Some research work[4,22,23] has suggested that the proteins can influence crystal nucleation, growth, and aggregation of calcium oxalate within the urinary system.

It was also believed that[3,16,24−26] the modification of crystal growth and crystal habit was achieved by the absorbance and binding of the proteins to the surface of CaOx. These adsorbed macromolecules can promote heterogeneous nucleation by attracting calcium ions to their calcium-binding domains at the surfaces.[16,25] Nevertheless, there is no concrete data to support those arguments. Apart from this, we notice that, to date, although some aspects of nucleation, growth, and aggregation of CaOx crystals in vitro have been studied including the effect of some human proteins,[7,27] no detailed studies on the crystallization of calcium oxalate crystals have been reported to elucidate the effect of these proteins. Evidently, an unambiguous understanding of the effects of these proteins on the formation of CaOx should be developed.

Recently, the structural synergy between biominerals and biosubstrates was examined. To that end particular emphasis was placed on the templating effect of the substrate as well as a newly identified supersaturation-driven interfacial structure mismatch effect in the context of a new nucleation model.[23,28−33] On the basis of this new nucleation model, some exciting results have been achieved in studying ice, calcium carbonate, and hydroxyapatite,[23,29,30] through a comparative analysis of the effects of various selected additives (salts, proteins, and other biopolymers). To obtain a better understanding of the CaOx crystallization and the role of the protein (albumin) in the urine, in this work, we employ the aforementioned model to examine the nucleation of COM and the impact of bovine serum albumin (BSA). In addition, we also examine how the protein (BSA) influences the assembly of CaOx from the kinetics point of view. Our aim is to identify an effective approach to control the formation of CaOx crystals and contribute to the treatment of kidney stones.

Experimental Section

Stock solutions were prepared by dissolving reagent-grade calcium chloride dihydrate ($CaCl_2 \cdot 2H_2O$, J.T. Baker), and sodium oxalate ($Na_2C_2O_4$, Merck) in deionized water. The pH was adjusted to 6.0. A series of concentrations, ranging from 3.6 to 5.2 mM, of the two solutions was prepared by gradually diluting the stock solutions. Both kinds of solutions were injected through filters (200 nm) into a rectangular glass cell to examine the kinetics of calcium oxalate formation from the reactants. The nucleation kinetics was examined by using dynamic light-scattering (DLS) employing a Brookhaven BI-200SM light-scattering system with a He−Ne laser (632.8 nm) source.[29] This system can detect particles of down to 2 nm, which allows an in situ measurement of the nucleation process and the size increase of the nuclei. The induction time t_s was measured by monitoring the photon count rate recorded by the DLS equipment against time. Subsequently, the effect of BSA (Sigma Chemicals) on the nucleation and the aggregation of calcium oxalate was also studied. Being synthesized by the liver and the main protein of plasma, albumin is a well-characterized protein[3,7,10,14,19,21] having a molecular weight 6.9×10^4 Da, a size of $11.6 \times 2.7 \times 2.7$ nm^3, an isoelectric point of 4.7−4.9,

* Author to whom correspondence should be addressed. E-mail: phyliuxy@nus.edu.sg.

10.1021/jp057403b CCC: $33.50
Published on Web 04/20/2006

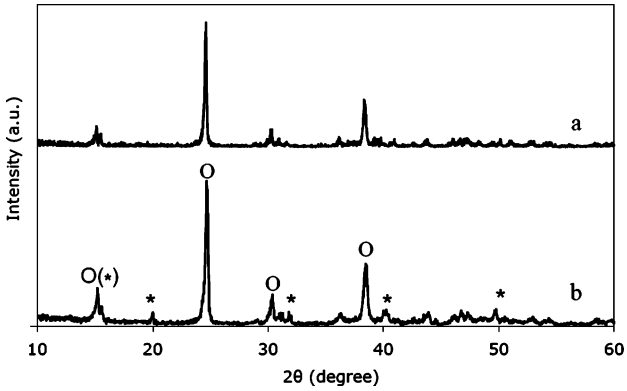

Figure 1. XRD patterns of CaOx crystals obtained from a solution with/without BSA. The crystal faces with open circles indicate the presence of COM. The asterisks indicate the presence of COD crystals: curve a, no additive; curve b, BSA present.

and a good binding capacity for water and Ca^{2+}. The experiment was carried out at the temperature of 25 °C.

To confirm the crystal phases of the samples, X-ray diffraction (Philips, PW 1729) analyses were carried out. The X-ray diffraction (XRD) patterns obtained were compared with those of calcium oxalate crystals listed in the powder diffraction database of the Joint Committee on Powder Diffraction Standards (JCPDS). To examine the morphology change of CaOx, the microstructure of the calcium oxalate assembly obtained under different conditions was observed using a scanning electron microscope (JSM-6700F, JEOL) after coating with platinum to increase the conductivity.

Results and Discussion

According to the JCPDS database, calcium oxalate monohydrate has monoclinic symmetry and belongs to the $P2_1/c$ space group with parameters $a = 6.29$, $b = 14583$, $c = 10.116$, and $\beta = 109.46$, while calcium oxalate dihydrate (COD) has tetragonal symmetry and belongs to the $I4/m$ space group with parameters $a = 12.35$ and $c = 7.363$. COM is thermodynamically more stable than COD.

The crystal phases of the samples prepared in this study were confirmed by XRD analyses. The XRD diffraction pattern (Figure 1) shows that in the presence of BSA the product is a mixture of calcium oxalate monohydrate and calcium oxalate dihydrate. The peak intensity showed that in the product the majority was COM and only a small portion was COD. However, the COM crystal was the only product once the BSA was removed. This indicates that BSA favors the formation of COD. As COD is less likely to adhere to renal tubular cells and is less injurious to cell membranes than COM is,[4,16] we concluded that BSA protects against stone formation.

In the following, we first focus on the nucleation kinetics of COM, as the initial step of crystallization is nucleation. That is a kinetic process by which embryos overcome the nucleation barrier ΔG^* to reach a critical radius r_c and develop to become crystals by a positive thermodynamic driving force $\Delta\mu/kT$. The supersaturation σ provides the driving force and can be given[23,29,31] by

$$\ln(1+\sigma) = \Delta\mu/kT = \ln(a/a_e) \tag{1}$$

Here k is the Boltzmann's constant, T is temperature, a and a_e are the actual and equilibrium activities of a given ion, respectively

$$\Delta\mu = kT \ln\frac{[a(Ca^{2+})][a(C_2O_4^{2-})]}{K_{sp}(COM)} \tag{2}$$

Here K_{sp}(COM) is the solubility product at a given temperature, and Ca^{2+}, $C_2O_4^{2-}$, and COM denote, respectively, the calcium ion, oxalate ion, and calcium oxalate. Through the use of eqs 1 and 2, the supersaturation, σ, can be calculated for different solution conditions.

Taking into account the effect of the substrate on both the nucleation barrier and the transport process, the nucleation induction is given as[28,31]

$$J = (R^s)^2 N^0 f(m)[f(m)]^{1/2} B \exp\left[-\frac{\Delta G^*_{homo}}{kT} f(m)\right] \tag{3}$$

with

$$f(m) = \Delta G^*_{hetero}/\Delta G^*_{homo} \tag{4}$$

where R^s and N^0 are the radius and the density of the substrates, respectively, B is the kinetic constant, Ω is the volume of the growth units, m relates to the interaction and (statistical) interfacial structural match between the crystalline phase and the foreign bodies, ΔG^*_{homo} is the homogeneous nucleation barrier, and ΔG^*_{hetero} is the heterogeneous nucleation barrier. The factor $f(m)$ describes the ability to lower the nucleation barrier ΔG^* due to the occurrence of foreign bodies and varies from 1 to 0. It is important because it can determine the heterogeneous nucleation barrier ΔG^*_{hetero}. As $f(m) \rightarrow 0$, ΔG^*_{hetero} vanishes almost completely, implying that the growing crystals are well oriented and ordered with respect to the structure of the substrate. While in the case of $f(m) \rightarrow 1$, the substrate exerts almost no influence on the nucleation, and the nucleation is controlled by the kinetics of homogeneous nucleation, which results in nuclei emerging disordered.[23,29,31,34] The influence of foreign particles such as dust particles, proteins, or even existing crystallites etc. on the nucleation barrier and the association between the nucleating phase and the substrate can be fully characterized by this factor.

To describe the kinetics of nucleation, one of the most common ways is to measure the nucleation induction time (t_s) at different supersaturations. The nucleation rate J can be defined[23,28−33] as $J \cong 1/(t_s V)$, where V is the volume of the system. Then from eq 3 then, we have

$$\ln t_s = \frac{\kappa f(m)}{[\ln(1+\sigma)]^2} - \ln\{V(R^s)^2 N^0 f''(m)[f(m)]^{1/2} B\} \tag{5}$$

where $\kappa = 16\pi\gamma_{cf}^3\Omega^2/3(kT)^3$, which will remain constant under a given condition.

Since for the crystalline phase m and $f(m)$ take on only certain values corresponding to some crystallographically preferred orientations, we expect a discrete set of intercepting straight lines from the $\ln(t_s)$ versus $1/[\ln(1+\sigma)]^2$ plot according to eq 5. These lines with different slopes, $\kappa f(m)$, indicate that nucleation is governed by a sequence of progressive heterogeneous processes. Apart from supersaturation, the role of the substrate is another important factor that influences the interfacial properties. Although the occurrence of a substrate will promote nucleation by providing templating, it will also reduce the effective collision of structural units to the surfaces of clusters, which slows down the nucleation kinetics.[23,31]

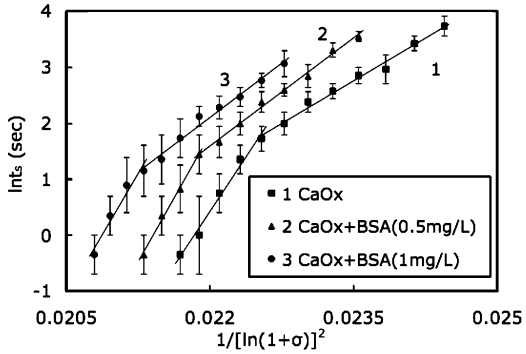

Figure 2. Plot of ln t_s(sec) vs $1/[\ln(1 + \sigma)\}]^2$ for calcium oxalate crystal nucleation under different conditions: curve 1, no additive; curve 2, with BSA at 0.5 mg/L; curve 3, with BSA at 1 mg/L.

To examine the influence of the supersaturation and the templating effect of the substrate on the nucleation kinetics and the subsequent structure correlation between calcium oxalate crystallites, the $\ln(t_s)$ versus $1/[\ln(1 + \sigma)]^2$ plots were constructed for calcium oxalate when BSA was fixed at a series of concentrations, as presented in Figure 2. According to eq 5, for a given system (κ, B = constant), we can analyze the change of the structure correlation between the substrate and the crystalline phase in terms of the variation of the slope of these plots. As shown in Figure 2, each of these depicted curves can in principle be fit by two intersecting straight lines with different slopes. This indicates that the nucleation is controlled by two discrete values of $f(m)$ within the corresponding regions. As the supersaturation increases, $f(m)$ increases sharply. This implies that the structural match between the substrate and the nucleating crystallites deteriorates as the supersaturation increases.

In the following, we will discuss how BSA enhanced the nucleation process of COM. First, let us review the general nucleation process: The growth units (molecules or ions) in the solution may, on collision, join into groups of two or more particles to form embryos. To reach a thermodynamically stable state, the embryos must overcome the nucleation energy barrier, thus attaining the "growth" of embryos.[29,31−33] During the growth of an embryo, growth units should be transported from the bulk solution to the surface of the embryo and become incorporated into the kink sites. However, when foreign bodies (impurities and/or protein molecules) are present, they become incorporated on the nucleus surface. This not only suppresses the nucleation barrier but also affects the transport of growth units to the surfaces of the crystalline clusters.[23,28,30] As shown in Figure 3A, the foreign body causes a reduction in the "effective surface" of the nucleus, that would normally be available for the growth units to incorporate themselves into the nucleus. This tends to slow the nucleation kinetics[23,29−31] and increase the nucleation induction time.

Actually, during the embryo growth, the solvent and foreign bodies that have been absorbed on both the kink sites and the surfaces of the growth units need to be desolvated. Here, let us define ΔG^+_{kink} to be the kink kinetics energy barrier, which must be overcome to remove solvent molecules absorbed at the kink sites, and $(\Delta G^+_{kink}{}')_{add}$ to be the kink kinetics energy barrier, which must be overcome to remove the absorbed foreign bodies at the kink sites. Obviously, the adsorption of foreign bodies on the surface of the crystal embryo, in particular at the kink sites, will enhance the kink kinetics energy barrier by $\Delta(\Delta G^+_{kink})_{add}$, which equals $(\Delta G^+_{kink}{}')_{add} - \Delta G^+_{kink}$ (Figures 3B and 3C). Consequently, the integration of growth units into crystal nuclei at the kink site will be significantly slowed or

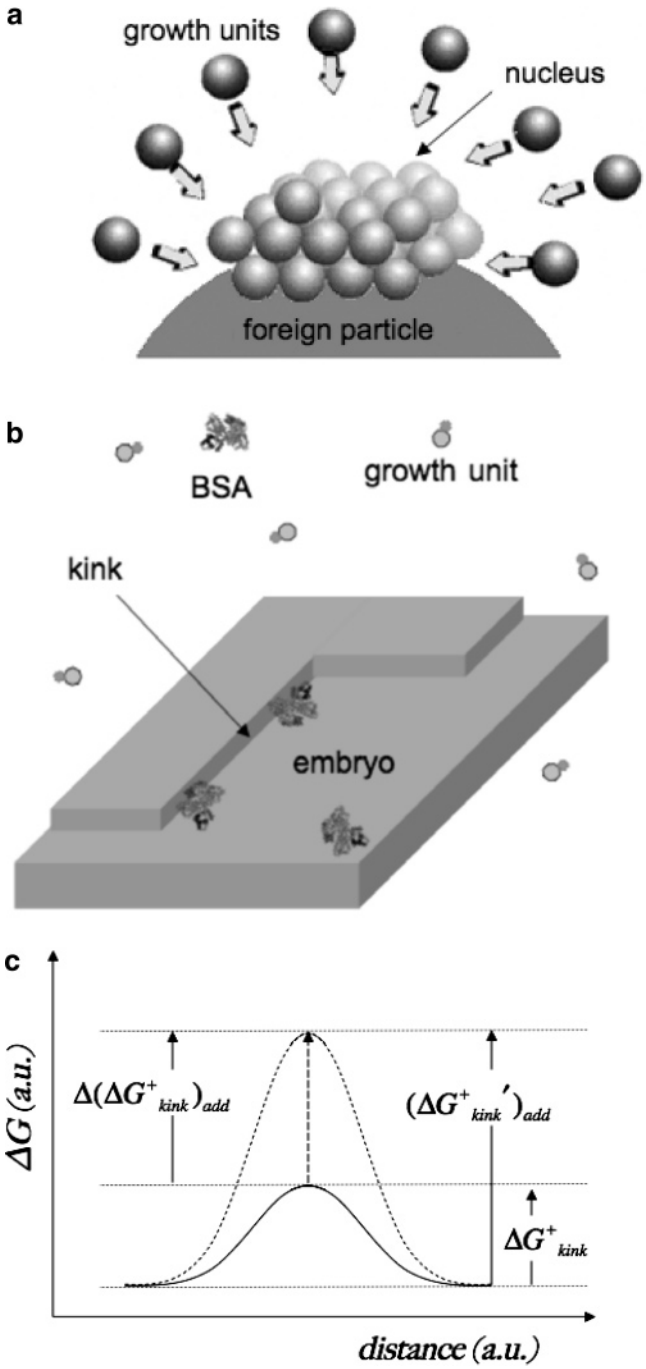

Figure 3. (A) Schematic illustration of the effect of foreign particles on the transport of structural units from the bulk to the nucleating site. The presence of the substrate reduces the effective surface of the nucleus. (B) Illustration of adsorption of BSA molecules at the kink site. In the process of nucleation, the adsorption of additives at the kink sites suppresses the approach of growth units to the embryo. (C) In the process of nucleation, the adsorption of additives at the kink site enhances the kink kinetics barrier by $\Delta(\Delta G^+_{kink})_{add} = (\Delta G^+_{kink}{}')_{add} - \Delta G^+_{kink}$.

even terminated due to the increase of the kink kinetics energy barrier.[23,28,30]

In our experiment, the presence of BSA inhibits crystal nucleation by absorbing at the kink sites. Thus, it increases the kink kinetics energy barrier and the induction time. According to refs 30 and 31, in Figure 2, the vertical distance of the straight lines along the y-axis equals $\Delta(\Delta G^+_{kink})_{add}/kT$, from which we can calculate the change of the kink kinetics energy barrier $\Delta(\Delta G^+_{kink})_{add}$. We calculated this equation for $[Ca^{2+}]$ =

$[C_2O_4^{2-}] = 2.1$ mM, in the presence of BSA at the concentrations of 0.5 and 1 mg/L, and we found that the energy barrier increase with reference to the case of homogeneous nucleation (where BSA is absent) is $0.62kT$ and $1.07kT$, respectively. When $[Ca^{2+}] = [C_2O_4^{2-}] = 2.35$ mM, the energy barrier increase from homogeneous nucleation to nucleation in the presence of BSA of 0.5 mg/L is $1.18kT$. However, when $[Ca^{2+}] = [C_2O_4^{2-}] = 2.45$ mM, the energy barrier increase for an increase in the BSA concentration from 0.5 to 1 mg/L is $1.18kT$.

The supersaturation at which $f(m)$ changes is defined as σ^*. A larger σ^* implies that good crystalline alignment will be achieved in a wider range of supersaturations.[23] In Figure 2, σ^* for curve 1, 2, and 3 is 7.01×10^2, 8.6×10^2, and 9.4×10^2, respectively, so that σ^* exhibits a monotonic increase with BSA concentration. This implies that the presence of BSA plays a crucial role in suppressing the supersaturation-driven structure mismatch effect occurring in the crystalline assembly over a wide range of supersaturations. Since BSA can prolong the range of supersaturation for a good structural match, we deduce from the above nucleation kinetics discussion that a better calcium oxalate crystallization assembly could be obtained in the presence of BSA. This conclusion was confirmed by recording the SEM micrographs shown in Figure 4.

The SEM micrographs confirm the conclusions obtained from the nucleation kinetics discussion. Figure 4A is the SEM picture of COM obtained from a solution at low concentration ($[Ca^{2+}] = [C_2O_4^{2-}] = 0.2$ mM) without additives. However, in the presence of BSA, no crystals were found even when all of the other conditions, such as supersaturation, pH, and temperature, were kept unchanged. Thus we arrived at the same conclusion as in the previous discussion obtained by the nucleation kinetics results, namely, that BSA inhibits the nucleation and the crystal growth of CaOx. Figure 4B is the SEM picture of randomly oriented COM crystals obtained from a solution at a high concentration ($[Ca^{2+}] = [C_2O_4^{2-}] = 0.35$ mM) without BSA. It shows a distorted morphology[35] as the crystals are highly aggregated. Meanwhile, the samples obtained in the same conditions as those in Figure 4B, except for the presence of BSA, are shown in Figure 4C. The image shows a good structure match and the coincident formation of COD and COM. This proves that the presence of BSA can prolong the range of supersaturation for a good structural match and achieve a better crystal assembly. Also the conclusion from the XRD analysis that the presence of BSA favors the formation of COD is confirmed.

As urinary stone formation is a time-restricted process, increasing the induction time may allow the crystals to remain small enough to be excreted out freely.[4] Moreover, COD and COM crystals differ in their ability to adhere to the wall of the kidney and/or renal tubule. As a consequence COD can be expelled out by the urine more easily than COM can, and COM is retained in the urinary system and induces the formation of urine stones.[3,4,16] Therefore, COD is less harmful to the human body than COM, and the presence of BSA could reduce the danger of urine stone formation. This process is illustrated by Figure 5.

Conclusions

In our investigation, a new nucleation model is employed in studying the nucleation of COM under the influence of BSA. The results show that the BSA protein not only inhibits the nucleation of COM by increasing the kink kinetics barrier but also promotes the structure synergy match between the protein and the substrates and favors the formation of COD. This study

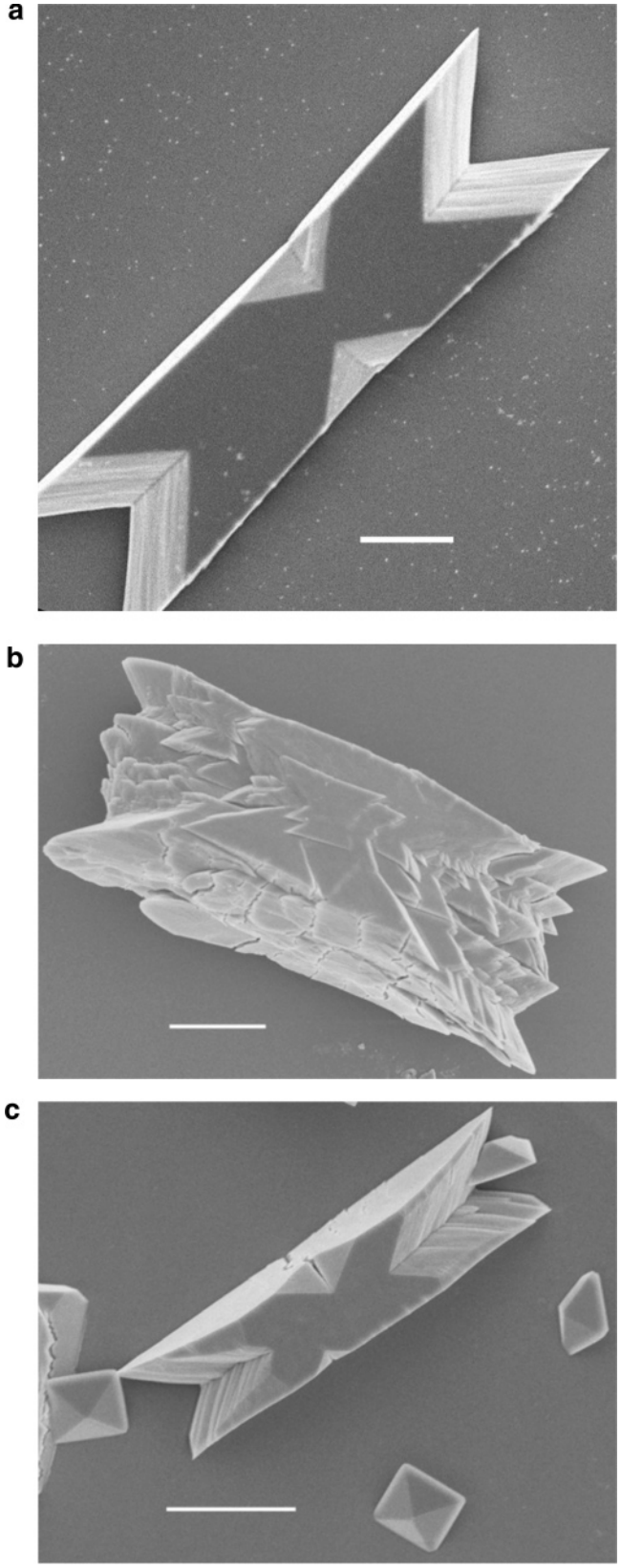

Figure 4. (A) SEM picture of COM twin crystals obtained from a solution at a low concentration ($[Ca^{2+}] = [C_2O_4^{2-}] = 0.2$ mM) without additives: scale bar, 5 μm. (B) SEM micrograph showing COM crystallites obtained from a solution at a high concentration ($[Ca^{2+}] = [C_2O_4^{2-}] = 0.35$ mM) without additives: scale bar, 5 μm. (C) SEM micrograph showing COM and COD crystallites obtained from a solution at a high concentration ($[Ca^{2+}] = [C_2O_4^{2-}] = 0.35$ mM), where BSA is used as an additive. Because of the templating effect of BSA, the crystallites show good structural synergy: scale bar, 5 μm.

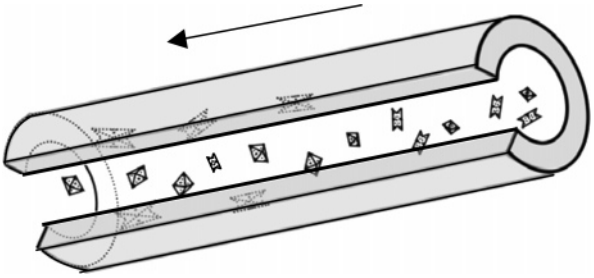

Figure 5. Scheme showing a renal tubule, in which supersaturated urine with CaOx is flowing. The arrow indicates the flow direction of the urine. In the urine, after the nucleation and growth of CaOx, most of the COM is bonded to the renal tubule, while most of the COD is propelled out.

also predicts the potential application of the BSA protein to the cure of urine stone disease.

Acknowledgment. The authors appreciate Janaky Narayanan for her help with this work.

References and Notes

(1) Nancollas, G. H.; Gardner, G. L. *J. Cryst. Growth* **1974**, *21*, 267.
(2) Girija, E. K.; Latha, S. C.; Kalkura, S. N.; Subramanian, C.; Ramasamy, P. *Mater. Chem. Phys.* **1998**, *52*, 253.
(3) Cerini, C.; Geider, S.; Dussol, B.; Hennequin, C.; Daudon, M.; Veesler, S.; Nitsche, S.; Boistelle, R.; Berthézène, P.; Dupuy, P.; Vazi, A.; Berland, Y.; Dagorn, J.-C.; Verdier, J.-M. *Kidney Int.* **1999**, *55*, 1776.
(4) Khan, S. R. *Calcium Oxalate in Biological Systems*; CRC Press: Boca Raton, FL, 1995.
(5) Francesch, V. R.; Nakata, P. A. *Annu. Rev. Plant Biol.* **2005**, *56*, 41.
(6) Joseph, K. C.; Parekh, B. B.; Joshi, M. J. *Curr. Sci.* **2005**, *88*, 1232.
(7) Grover, P. K.; Moritz, R. L.; Simpson, R. J.; Ryall, R. L. *Eur. J. Biochem.* **1998**, *253*, 637.
(8) Grover, P. K.; Ryall, R. L.; Marshall, V. R. *Clin. Chim. Acta* **1990**, *190*, 129.
(9) Yoshioka, T.; Koide, T.; Utsunomiya, M.; Itatani, H.; Oka, T.; Sonoda, T. *Br. J. Urol.* **1989**, *64*, 463.
(10) Ryall, R.; Harnett, R. M.; Hibberd, C. M.; Edyvane, K. A.; Marshall, V. R. *Urol. Res.* **1991**, *19*, 181.
(11) Nakagawa, Y.; Ahmed, M.; Hall, S. L.; Deganello, S.; Coe, F. L. *J. Clin. Invest.* **1987**, *79*, 1782.
(12) Worcester, E. M.; Sebastian, J. L.; Hiatt, J. G.; Beshensky, A. M.; Sadowski, J. A. *Calcif. Tissue Int.* **1993**, *53*, 242.
(13) Tang, Y.; Grover, P.; Moritz, R.; Simpson, R.; Ryall, R. *Br. J. Urol.* **1995**, *76*, 425.
(14) Baumann, J. M.; Affolter, B.; Caprez, U.; Henze, U. *Eur. Urol.* **2003**, *43*, 421.
(15) Konya, E.; Umekawa, T.; Iguchi, M.; Kurita, T. *Eur. Urol.* **2003**, *43*, 564.
(16) Ryall, R. L.; Chauvet, M. C.; Grover, P. K. *BJU Int.* **2005**, *96*, 654.
(17) Reinhold, F. P.; Hultenby, K.; Oldberg, Å.; Heinegård, D. *Proc. Natl Acad. Sci. U.S.A.* **1990**, *87*, 4473.
(18) Brown, L. F.; Berse, B.; Van de Water, L.; Papadopoulos-Sergiou, A.; Perruzzi, C. A.; Manseau, E. J.; Dvorak, H. F.; Senger, D. R. *Mol. Biol. Cell* **1992**, *3*, 1169.
(19) Nancollas, G. H.; Wu, W. *J. Cryst. Growth* **2000**, *211*, 137.
(20) Jung, T.; Kim, W.-S.; Choi, C. K. *Mater. Sci. Eng., C* **2004**, *24*, 31.
(21) Wassell, D. T. H.; Hall, R. C.; Embery, G. *Biomaterials* **1995**, *16*, 697.
(22) Combes, C.; Rey, C. *Biomaterials* **2002**, *23*, 2817.
(23) Jiang, H.; Liu, X.-Y. *J. Biol. Chem.* **2004**, *279*, 41286.
(24) Jauregui-Zuniga, D.; Reyes-Grajeda, J. P.; Moreno, A. *Plant Sci.* **2005**, *168*, 1163.
(25) Asokan, D.; Kalaiselvi, P.; Farooq, S. M.; Varalakshmi, P. *Urol. Res.* **2004**, *32*, 357.
(26) Jung, T.; Sheng, X.; Choi, C. K.; Kim, W.-S.; Wesson, J. A.; Ward, M. D. *Langmuir* **2004**, *20*, 8587.
(27) El-Shall, H.; Jeon, J.-h.; Abdel-Aal, E. A.; Khan, S.; Gower, L.; Rabinovich, Y. *Cryst. Res. Technol.* **2004**, *39*, 222.
(28) Liu, X. Y. *J. Chem. Phys.* **2000**, *112*, 9949.
(29) Liu, X. Y.; Lim, S. W. *J. Am. Chem. Soc.* **2003**, *125*, 888.
(30) Du, N.; Liu, X. Y.; Hew, C. L. *J. Biol. Chem.* **2003**, *278*, 36000.
(31) Liu, X. Y. *J. Phys. Chem. B* **2001**, *105*, 11550.
(32) Liu, X. Y. *J. Cryst. Growth* **2002**, *237*, 1806.
(33) Liu, X. Y. *Surf. Rev. Lett.* **2001**, *8*, 415.
(34) El-Shall, H.; Jeon, J.-h.; Abdel-Aal, E. A.; Khan, S.; Gower, L.; Rabinovich, Y. *Cryst. Res. Technol.* **2004**, *39*, 214.
(35) Walton, R. C.; Kavanagh, J. P.; Heywood, B. R. *J. Struct. Biol.* **2003**, *143*, 14.